

# Electron-phonon interaction in small-radius carbon nanotubes

Ryan Barnett, Eugene Demler, and Efthimios Kaxiras  
*Department of Physics, Harvard University, Cambridge MA 02138*  
(Dated: May 22, 2019)

We perform analysis of the band structure, phonon dispersion, and electron-phonon interactions in ultrasmall (5,0) nanotubes. The large curvature makes these tubes metallic with a large density of states at the Fermi energy and leads to unusual electron-phonon interactions, with the dominant coupling coming from the out-of-plane phonon modes. By combining the frozen-phonon approximation with the RPA analysis of the giant Kohn anomaly in 1d we find parameters of the effective Frölich Hamiltonian for the conduction electrons and discuss possible instabilities of the electron-phonon system. We argue that the  $2k_F$  charge-density wave dominates over the superconducting electron pairing and should open a pseudogap for quasiparticles at a temperature around 160 K.

The discovery of carbon nanotubes [1] has lead to a renewed interest in the study of 1d electron systems. The difference between semiconducting and metallic large-radius nanotubes may be typically understood by quantizing the circumferential momentum of the electronic states in a single graphite layer (see, for instance, [2]). Less conventional properties of nanotubes include Luttinger liquid behavior of metallic nanotubes found in tunneling experiments (see [3] and references therein), Coulomb effects [4], Kondo physics [5], and intrinsic superconductivity observed in ropes [6] and small-radius nanotubes in a zeolite matrix [7]. The findings motivated theoretical analysis of electron-phonon coupling (EPC) in carbon nanotubes, including studies of charge-density wave (CDW) [8, 9, 10] and superconducting [11, 12, 13, 14, 15] instabilities. Most theoretical analyses of electron-phonon interactions in nanotubes assume the phonon frequencies to be the same as in graphite and calculate the electron-phonon coupling strength from a simplified tight-binding model for the  $\pi$  orbitals of the C atoms. Such an approach, however, may not be suited for ultrasmall nanotubes (such as the ones in [7]), for which the curvature of the nanotube leads to strong hybridization of the  $\sigma$  and  $\pi$  orbitals, which results in a qualitatively different band structure [17], phonon spectrum, and electron-phonon interactions.

In this letter we present calculations of the band structure and EPC for small-radius (5,0) nanotubes and discuss possible CDW and superconducting instabilities in this system. We demonstrate that even though standard electronic structure approaches for calculating phonon frequencies, such as the frozen-phonon approximation (FPA), run into divergencies intrinsic to mean-field calculations in 1d, they can be analyzed from the point of view of the random-phase approximation (RPA) for the electron-phonon system and parameters of the effective Frölich Hamiltonian can be extracted. The main results that we obtain are: (i) The strongest electron-phonon interaction in the small-radius (5,0) nanotubes occurs for the out-of-plane phonon modes, unlike the case of graphite and larger radius nanotubes for which in-plane phonon modes dominate; (ii) Within the RPA, we ob-

tain a CDW transition temperature of  $T_0 = 160$  K [25]. In a 1d system we may not have a true phase transition at finite temperature, although we expect a quasiparticle pseudogap to appear at  $T_0$ ; (iii) The wave vector of the leading CDW instability  $2k_F \approx 0.22\frac{2\pi}{a}$  (where  $a$  is the length of a unit cell) is incommensurate, and we expect that in an ideal nanotube, quantum fluctuations should destroy long-range CDW order even at  $T = 0$ . However, pinning on impurities, lattice defects, and boundaries may stabilize CDW order locally, leading to insulating behavior at low temperatures; (iv) Using the bare phonon frequencies we obtain an electron-phonon coupling  $\lambda = 0.56$ , which gives a mean-field superconducting transition temperature  $T_{SC} = 26$  K. We argue, however, that the superconducting instability is suppressed by opening the CDW pseudogap even when enhancement of  $\lambda$  due to softening of the phonon modes is taken into account.

To compute the electronic structure of a (5,0) carbon nanotube, we use the NRL tight-binding method [16] which has been tested extensively and provides accurate results on a variety of materials. In agreement with previous calculations for zig-zag nanotubes [17][18], we find that the bonds along the tube axis contract ( $d_1 = 1.420$  Å) while the bonds with a component along the perimeter of the tube expand ( $d_2 = 1.445$  Å) compared to the graphitic value ( $d_0 = 1.425$  Å). With this relaxed structure, the band structure was calculated and is shown in Fig 1. While simple graphite zone-folding arguments predict the nanotube to be insulating, the band structure clearly exhibits metallic behavior. The inner band (with the smaller  $k_F^\sigma$ ) is doubly degenerate and originates from the  $\sigma$  bonds in graphite while the outer band (with the larger  $k_F^\pi$ ) is nondegenerate and originates from the  $\pi$  bonds in graphite. An exact relation  $2k_F^\sigma = k_F^\pi$  holds for the tubes that have the same electron density as in graphite. The failure of the zone-folding procedure is due to the strong curvature effects, which lead to considerable band shifts in small-radius nanotubes, as discussed originally in [17] for (6,0) nanotubes based on density-functional theory calculations. As a result of these band shifts, for the (5,0) nanotubes we have a system close to a

Van Hove singularity for the  $\sigma$  band which has a density of states of 0.16 states/eV per C atom. For comparison, the density of states for the (5,5) nanotubes is only 0.028 states/eV per C atom, so we expect that instabilities of the electron-phonon systems for the (5,0) nanotubes are strongly enhanced compared to larger radius nanotubes.

The standard (Frölich) Hamiltonian for the conduction electrons interacting with phonons is given by

$$\mathcal{H} = \sum_{k\tau\sigma} \epsilon_{k\tau} c_{k\tau\sigma}^\dagger c_{k\tau\sigma} + \sum_{q\mu} \Omega_{q\mu}^0 (a_{q\mu}^\dagger a_{q\mu} + \frac{1}{2}) + \sum_{k\tau k'\tau'\sigma\mu} g_{k\tau k'\tau'\mu} c_{k\tau\sigma}^\dagger c_{k'\tau'\sigma} (a_{q\mu} + a_{-q\mu}^\dagger). \quad (1)$$

Here  $c_{k\tau\sigma}^\dagger$  creates an electron with quasimomentum  $k$  in band  $\tau$  with spin  $\sigma$ ,  $a_{q\mu}^\dagger$  creates a phonon with lattice momentum  $q$  and polarization  $\mu$ , and  $q = k - k'$  modulo a reciprocal lattice vector. The energies of electron quasiparticles and phonons (in the absence of EPC) are given by  $\epsilon_{k\tau}$  and  $\Omega_{q\mu}^0$  respectively. The EPC vertex is given by

$$g_{k\tau k'\tau'\mu} = \sqrt{\frac{\hbar}{2\Omega_{q\mu}^0 M N N_c}} M_{k\tau k'\tau'\mu} \quad (2)$$

with  $M_{k\tau k'\tau'\mu} = N \langle \psi_{k\tau} | \sum_i \frac{\delta V}{\delta \mathbf{R}_{0i}} \cdot \hat{\epsilon}_{q\mu}(i) | \psi_{k'\tau'} \rangle$ . Here  $|\psi_{k\tau}\rangle$  is a quasistationary electron state in band  $\tau$  with quasimomentum  $k$ ,  $\hat{\epsilon}_{q\mu}(i)$  is the phonon polarization vector on atom  $i$  in the unit cell,  $N_c$  is the number of atoms per unit cell,  $M$  is the mass of a single C atom,  $N$  is the total number of unit cells in the system, and  $\frac{\delta V}{\delta \mathbf{R}_{0i}}$  is the derivative of the crystal potential with respect to the ion position  $\mathbf{R}_{0i}$ . The matrix element  $M_{k\tau k'\tau'\mu}$  may be calculated by perturbing the lattice potential by  $\delta \mathbf{R}_{ni} = ue^{iqR_n} \hat{\epsilon}_{q\mu}(i)$  as  $M_{k\tau k'\tau'\mu} = \frac{1}{u} \langle \psi_{k\tau} | (V^{q\mu} - V_0) | \psi_{k'\tau'} \rangle$  which was originally shown in [19] where a method for calculating  $M_{k\tau k'\tau'\mu}$  with a plane-wave basis set was developed. Using the tight-binding basis set, we have

$$M_{k\tau k'\tau'\mu} = \frac{1}{u} \sum_{ilil'} A_{k\tau il}^* \langle \chi_{kil}^{q\mu} | (\mathcal{H}^{q\mu} - E_F) | \chi_{k'i'l'}^{q\mu} \rangle A_{k'\tau'i'l'} \quad (3)$$

for the coupling between two states  $k\tau$  and  $k'\tau'$  on the Fermi surface where  $i, i'$  are summed over atoms in the unit cell and  $l, l'$  are summed over basis orbitals. Here  $\mathcal{H}^{q\mu}$  is the Hamiltonian with the perturbed ionic potential  $V^{q\mu}$ ,  $|\chi_{kil}^{q\mu}\rangle$  are the tight-binding basis functions centered on the lattice perturbed by the phonon  $q\mu$ , and  $A_{k\tau il}$  are coefficients of the wavefunctions for the undistorted lattice  $|\psi_{k\tau}\rangle = \sum_{il} A_{k\tau il} |\chi_{kil}\rangle$ . We point out that it is sufficient to take  $|\chi_{kil}^{q\mu}\rangle$  instead of  $|\chi_{k'i'l'}^{q\mu}\rangle$  in Eq. (3) in the limit of a large unit cell [26].  $M_{k\tau k'\tau'\mu}$  can then be computed by evaluating the tight-binding Hamiltonian and overlap matrices for the distorted lattice and determining the coefficients  $A_{k\tau il}$  and  $A_{k'\tau'i'l'}$  of the wavefunctions for the undistorted lattice.

To obtain the phonon polarization eigenvectors, we use the  $6 \times 6$  dynamical matrix of graphite given in [20] which gives both in-plane and out-of-plane modes. We then use the zone-folding method to obtain the modes for the (5,0) nanotube. For each wave vector  $q = k - k'$  connecting Fermi points, we calculate  $M_{k\tau k'\tau'\mu}$  for each of the 60 ( $=20$  atoms/cell  $\times$  3 dimensions) modes  $\mu$ . The modes that have the largest EPC were found to be intraband processes along the  $\Gamma M$  line of graphite and are shown in Fig. 1. For the  $2k_F^\sigma$  intraband processes, the strongest EPC is to the out-of-plane optical mode followed by the out-of-plane breathing mode and an in-plane optical mode. For this process, there are several other modes not shown that have significant but smaller EPC. We also calculated non-negligible EPC for the interband processes, but these also were significantly smaller than the intraband processes. The modes relevant to intraband  $2k_F^\pi$  EPC are, in descending order, the out-of-plane optical mode, the in-plane optical mode, the out-of-plane breathing mode, and the in-plane acoustic mode which are the only processes which give nonzero coupling. The quantitative values for the coupling matrix elements will be reported in a future publication [21].

Previous calculations have relied on a simplified tight-binding model and predicted that only the in-plane phonon modes couple appreciably to the electrons. In contrast to this, our method shows that the most dominant coupling for a (5,0) tube is to the out-of-plane modes. This effect is unique for small-radius nanotubes, so already for the (5,5) tube our calculations agree qualitatively with the simplified tight-binding models [21].

Now we move on to the issue of how to calculate  $\Omega_{q\mu}^0$ . In the standard FPA [22], the frequencies are given by  $\Omega_{q\mu} = ((\Delta E_{cos} + \Delta E_{sin})/(MN_c))^{1/2}/u$ , where  $u$  is the amplitude of the displacement, and  $\Delta E_{cos}$  and  $\Delta E_{sin}$  are the energy differences per unit cell between the distorted and equilibrium lattice structures where the distortion corresponds to the real and imaginary parts of  $\delta \mathbf{R}_{ni} = ue^{iqR_n} \hat{\epsilon}_{q\mu}(i)$  respectively. The phonon dispersion curves obtained from the FPA for the (5,0) nanotube along the  $\Gamma M$  line are shown in Fig 2. For comparison, we show frequencies of these modes calculated by using the dynamical matrix of graphite [20]. Unit cell sizes of up to 400 atoms in increments of 20 (which is the number of atoms in the smallest possible unit cell) were used in the FPA, requiring the phonon wavevectors to be commensurate with the chosen supercell. The FPA results show good agreement with the graphitic values for the in-plane modes. The out-of-plane acoustic mode of graphite gets mapped to the radial breathing mode in the nanotube, which leads to significant differences in energy. However, the biggest renormalization from the graphitic mode (a) energy occurs for the optical out-of-plane mode that shows giant Kohn anomalies at  $2k_F^\sigma$  and  $2k_F^\pi$  [23].

It is important to realize that the divergence of  $\Omega_{q\mu}$  shown in Fig. 2 does not imply the divergence of  $\Omega_{q\mu}^0$  in

the Frölich Hamiltonian Eq. (1). In the FPA, the phonon frequencies are calculated *after* the electron-phonon interaction in Eq. (1) have been included, which gives anomalous softening at  $2k_F$  due to the well-known Peierls instability of electron-phonon systems in 1d. To extract the bare phonon frequency  $\Omega_{q\mu}^0$  from the numerically computed  $\Omega_{q\mu}$ , we point out a connection between the FPA and the RPA for the Frölich Hamiltonian. For negligible interband coupling (as is the case for the out-of-plane optical mode), the phonon propagator in the RPA is given by

$$D_\mu^{-1}(q, q_0) = D_{0\mu}^{-1}(q, q_0) - \sum_\tau |g_{k\tau k'\tau\mu}|^2 \Pi_{0\tau}(q, q_0) \quad (4)$$

where  $D_{0\mu}(q, q_0)$  is the bare phonon propagator and

$$\Pi_{0\tau}(q, q_0) = 2 \sum_p \frac{f_{p\tau} - f_{p+q,\tau}}{\hbar q_0 + \epsilon_{p\tau} - \epsilon_{p+q,\tau}} \quad (5)$$

is the electron polarizability where  $f_{p\tau}$  is the Fermi-Dirac distribution function. The poles of  $D_\mu(q, q_0)$ , which give the dressed phonon frequency  $\Omega_{q\mu}$ , satisfy the equation  $(\Omega_{q\mu})^2 = (\Omega_{q\mu}^0)^2 + \frac{2}{\hbar} \Omega_{q\mu}^0 \sum_\tau |g_{k\tau k'\tau\mu}|^2 \Pi_{0\tau}(q, \Omega_{q\mu})$ . The FPA corresponds to setting  $\Omega_{q\mu} \rightarrow 0$  in  $\Pi_{0\tau}(q, \Omega_{q\mu})$ , which is usually a good approximation due to the large difference between phonon and electron energies  $\Omega_{q\mu} \ll E_F$ . Our bands are approximated well by parabolas with effective masses  $m_\sigma^* = 0.58 m_e$  and  $m_\pi^* = 0.28 m_e$  which, at zero temperature, leads to:

$$\begin{aligned} (\Omega_{q\mu})^2 = & (\Omega_{q\mu}^0)^2 + |M_{2k_F^\sigma}|^2 \frac{2m_\sigma^* a}{\pi M N_c k_F^\sigma \hbar^2} \log \left| \frac{2k_F^\sigma - q}{2k_F^\sigma + q} \right| \\ & + |M_{2k_F^\pi}|^2 \frac{m_\pi^* a}{\pi M N_c k_F^\pi \hbar^2} \log \left| \frac{2k_F^\pi - q}{2k_F^\pi + q} \right| \end{aligned} \quad (6)$$

where we have written the EPC vertex in terms of the matrix elements  $M_{2k_F^{\sigma,\pi}}$  as defined in Eq. (2). We see that the frequency of a phonon with nonzero EPC goes to zero in the vicinity of  $q = 2k_F^{\sigma,\pi}$ . This is the celebrated Peierls instability to a CDW state.

In Fig. 2 we show that a simple quadratic fit for the bare phonon frequency  $(\Omega_{q\mu}^0)^2 = A + Bq + Cq^2$  in Eq. (6) gives a good match of the dispersion  $\Omega_{q\mu}$  with the values computed with the FPA for the out-of-plane optical mode which has the most dramatic divergence. It is seen that the curvature of the (5,0) nanotube leads to a significant renormalization of the bare phonon frequency  $\Omega_{q\mu}^0$ . This can be understood by comparing the two distinct bond angles in our structure of  $119.4^\circ$  and  $111.9^\circ$  with the  $sp^2$  and  $sp^3$  bond angles of  $120^\circ$  and  $109.4^\circ$  respectively. The out-of-plane optical mode oscillates between these two C bonding configurations which provides a qualitative explanation for the softening. We emphasize that we fit only the regular part of the phonon spectrum  $\Omega_{q\mu}^0$  and coefficients of the log divergencies at  $2k_F^\sigma$  and  $2k_F^\pi$  are

fixed by the effective mass  $m_{\sigma,\pi}^*$  and  $k_F^{\sigma,\pi}$  (known from the band structure) and the computed EPC matrix elements  $M_{2k_F^\sigma} = 5.55$  eV/Å and  $M_{2k_F^\pi} = 8.56$  eV/Å. Excellent agreement of the FPA with our model in the vicinity of the singular points provides a good self-consistency check for our analysis.

After finding parameters for the Hamiltonian in Eq. (1) we can now calculate the RPA transition temperature into the CDW phase and find  $T_0 = 4\epsilon_F \exp\{-\Omega_{2k_F^\sigma}^0 / (|g_{2k_F^\sigma}|^2 \nu(0))\} = 160$  K. Here  $\nu(0)$  is the contribution to the total density of states from the two degenerate inner bands which have the same coupling to the out-of-plane optical mode,  $\epsilon_F = \frac{k_F^{\sigma^2}}{2m_\sigma^*}$ , and  $\Omega_{2k_F^\sigma}^0$  is the bare phonon frequency extracted by the above method. Long range order may not appear in a 1d system at finite temperature, so the correct way to interpret  $T_0$  is by using the Landau-Ginzburg formalism [24]. We introduce a complex order parameter  $\Psi_1(x)$  related to the amplitude of the lattice distortion as  $q(x) = e^{2ik_F^\sigma x} \Psi_1(x) + e^{-2ik_F^\sigma x} \Psi_1^*(x)$ . At low temperature the free energy is given by  $F_\sigma[\Psi_1] = \int dx (a|\Psi_1|^2 + b|\Psi_1|^4 + c|\frac{d\Psi_1}{dx}|^2)$ . Below the mean-field transition temperature  $T_0$  we have  $a < 0$  and the system develops an amplitude for the order parameter  $\Psi_1$ . The phase of  $\Psi_1$ , however, is still fluctuating, leading to short range correlations for the CDW order  $\langle \Psi_1(x) \Psi_1^*(0) \rangle \propto e^{-x/\xi(T)}$ . Even at  $T = 0$  we can have at best a quasi long-range order for  $\Psi_1$  due to the incommensurate value of  $2k_F^\sigma$ . Lattice distortions at  $2k_F^\pi$  can be included by introducing another complex field  $\Psi_2(x)$  that contributes  $e^{2ik_F^\pi x} \Psi_2(x) + e^{-2ik_F^\pi x} \Psi_2^*(x)$  to the distortion amplitude. The relation  $2k_F^\sigma = k_F^\pi$  implies that the free energy allows coupling between  $\Psi_1$  and  $\Psi_2$  of the form  $F_{\pi\sigma}[\Psi_1, \Psi_2] = \gamma \int dx (\Psi_1^2 \Psi_2^* + \Psi_1^* \Psi_2^2)$ , so when the amplitude of  $\Psi_1$  is established, it will immediately induce the amplitude for  $\Psi_2$  (although none of the fields has a long-range order). Appearance of such amplitudes should lead to a pseudogap state of the system below  $T_0$  [24]. The dominant contribution to electrical conductivity in a clean system would then come from the Goldstone mode of the phase of the  $\Psi$ 's, i.e. sliding of CDWs (Frölich mode). Any kind of disorder (e.g. impurities or crystal defects), however, gives strong pinning of the CDW phase and suppresses collective mode contributions to transport. Therefore, we expect insulating behavior of the low temperature resistivity in most experimentally relevant circumstances.

We now discuss the superconducting pairing instability for the (5,0) nanotube. The electron-phonon coupling constant used in the BCS model is given by

$$\lambda = \frac{1}{\nu(0)} \sum_{(k\tau) \neq (k'\tau'), \mu} \delta(\epsilon_{k\tau}) \delta(\epsilon_{k'\tau'}) |g_{k\tau k'\tau'\mu}|^2 \frac{2}{\hbar \Omega_{q\gamma}}. \quad (7)$$

Here  $\nu(0)$  is the density of states at the Fermi level per spin and summation goes over all intra- and interband processes. In 3d systems phonon frequencies are only

weakly affected by the interaction with conduction electrons. However, in the case of 1d nanotubes, EPC leads to strong softening of the phonon frequencies which could imply strong enhancement of  $\lambda$  [23]. Using the *bare* phonon frequencies  $\Omega_{q\mu}^0$  in Eq. (7) corresponds to finding a *lower* bound for  $\lambda$ . Taking  $\Omega_q^0 = 433 \text{ cm}^{-1}$  for the out-of-plane optical mode at  $2k_F^\sigma$  in Eq. (7) we get  $\lambda = 0.56$ . Using the modified McMillan formula

$$T_{SC} = \frac{\langle \Omega \rangle}{1.20} \exp \left[ -\frac{1.04(1+\lambda)}{\lambda - \mu^*(1+0.62\lambda)} \right]. \quad (8)$$

with the average phonon frequency  $\langle \Omega \rangle = 1400 \text{ K}$  and the Coulomb pseudopotential  $\mu^* = 0.1$  [11] we get  $T_{SC} = 26 \text{ K}$ . The superconducting transition temperature which is lower than  $T_0$  is unphysical, since the pseudogap appearing in the quasiparticle spectrum below  $T_0$  leads to a strong suppression of superconducting pairing that is not captured by Eq. (8). To study the possibility that the giant Kohn anomaly (phonon softening) leads to such a dramatic renormalization of  $\lambda$  that  $T_{SC}$  becomes higher than  $T_0$ , we solved the self-consistent Eliashberg equations with the temperature dependent phonon frequency  $\Omega_{q\mu}(T)$  [21]. The temperature dependence of  $\Omega_{q\mu}$  was obtained from Eq. (6) using a finite temperature expression for the electron polarization  $\Pi_0(q, 0)$ . Within this procedure we did not find the superconducting instability above  $T_0$ . Hence, we conclude that superconductivity in (5,0) nanotubes should be suppressed by the opening of a pseudogap due to the CDW instability.

We thank C. Chamon, S. Das Sarma, L. Glazman, S. Kivelson, C. Marcus, I. Mazin, M. Mehl, A. Millis, M. Tinkham, and especially B. Halperin for very useful discussions. This work was supported by the NSF grant DMR-0132874 and by the Sloan foundation. RLB was partially supported by an NSF graduate research fellowship.

- [9] Y. Huang, M. Okada, K. Tanaka, and T. Yamabe, *Solid State Comm.* **97**, 303 (1996).
- [10] A. Sedeki, L. G. Caron, and C. Bourbonnais, *Phys. Rev. B* **62**, 6975 (2000).
- [11] L. X. Benedict, V. H. Crespi, S. G. Louie, and M. L. Cohen, *Phys. Rev. B* **52**, 14935 (1995).
- [12] A. Sedeki, L. G. Caron, and C. Bourbonnais, *Phys. Rev. B* **65**, 140515 (2002).
- [13] J. Gonzalez, *Phys. Rev. Lett.* **88**, 76403 (2002).
- [14] K. Byczuk, [condmat/0206086](#).
- [15] K. Kamide, T. Kimura, M. Nishida, and S. Kurihara, [condmat/0301115](#).
- [16] M. J. Mehl and D. Papaconstantopoulos, *Phys. Rev. B* **54**, 4519 (1996).
- [17] X. Blase, L. X. Benedict, E. L. Shirley, and S. G. Louie, *Phys. Rev. Lett.* **72**, 1878 (1994).
- [18] D. Sanchez-Portal, E. Artacho, J. Soler, A. Rubio, and P. Ordejon, *Phys. Rev. B* **59**, 12678 (1999).
- [19] P. Lam, M. Dacorogna, and M. Cohen, *Phys. Rev. B* **34**, 5065 (1986).
- [20] R. A. Jishi, L. Venkataraman, M. S. Dresselhaus, and G. Dresselhaus, *Chem. Phys. Lett.* **209**, 77 (1993).
- [21] R. Barnett, E. Demler, and E. Kaxiras, unpublished.
- [22] M. T. Yin and M. L. Cohen, *Phys. Rev. B* **26**, 5668 (1982).
- [23] A. J. Heeger in *Highly Conducting One-Dimensional Solids*, (Plenum Press, New York, 1979).
- [24] L. G. Caron in *Organic Conductors: Fundamentals and Applications*, (Marcel Dekker, New York, 1994).
- [25] We also computed the band structure of the (5,0) nanotube from first principles, and found it to be qualitatively similar. The first-principles results give a larger density of states at the Fermi energy which should lead to an even larger CDW transition temperature. However, because of the large unit cell sizes required to calculate the FPA frequencies and the EPC, the full first-principles treatment is unfeasable at this time.
- [26] The convergence as a function of supercell size was checked. Typically, we found supercell sizes of around 10 times the original unit cell were sufficient.

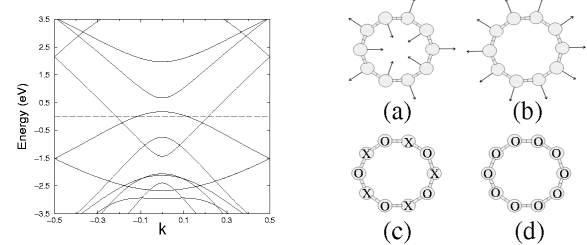


FIG. 1: Left: The band structure of a (5,0) nanotube where we set  $E_F = 0$ . Right: The phonon modes that have the strongest electron-phonon coupling. Shown is a cross-sectional slice of the nanotube containing 10 atoms. Modes (a), (b), (c), and (d) are out-of-plane optical, out-of-plane breathing, in-plane optical, and in-plane acoustic modes respectively. The X's and O's denote vectors in and out of the page.

- [1] S. Iijima, *Nature* **54**, 56 (1991).
- [2] R. Saito, G. Dresselhaus, and M. S. Dresselhaus, *Physical Properties of Carbon Nanotubes*, (Imperial College Press, London, 1998).
- [3] R. Egger, A. Bachtold, M. Fuhrer, M. Bockrath, D. Cobden, and P. McEuen, [cond-mat/0008008](#).
- [4] D. Cobden, M. Bockrath, P. McEuen, A. Rinzler, and R. Smalley, *Phys. Rev. Lett.* **81**, 681 (1998).
- [5] J. Nygard, D. Cobden, and P. Lindelof, *Nature* **408**, 342 (2000).
- [6] M. Kociak, A. Y. Kasumov, S. Gueron, B. Reulet, I. I. Khodos, Y. B. Gorbatov, V. T. Volkov, L. Vaccarini, and H. Bouchiat, *Phys. Rev. Lett.* **86**, 2416 (2001).
- [7] Z. Tang, L. Zhang, N. Wang, X. Zhang, G. Wen, G. Li, J. Wang, C. Chan, and P. Sheng, *Science* **292**, 2462 (2001).
- [8] J. Mintmire, B. Dunlap, and C. White *et al.*, *Phys. Rev. Lett.* **68**, 631 (1992).

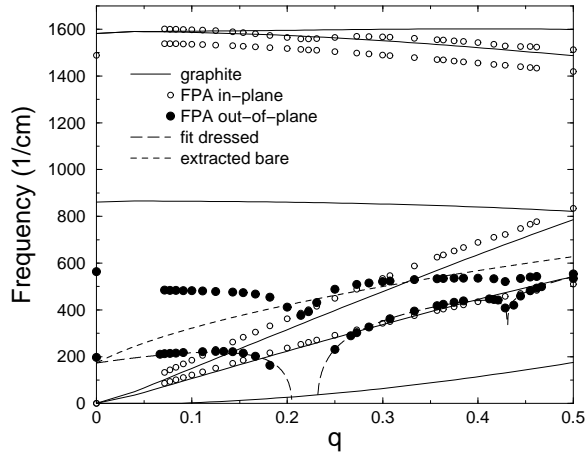


FIG. 2: The phonon dispersion along the  $\Gamma M$  line of the first Brillouin zone of graphite showing logarithmic divergences at  $2k_F^{\sigma,\pi}$ . The out-of-plane optical mode FPA frequencies are fit by  $\Omega_{q\tau}$  from Eq. (6).